J Geogr Syst (2012) 14:463–483
DOI 10.1007/s10109-012-0166-z

ORIGINAL ARTICLE

Understanding intra-urban trip patterns from taxi trajectory data

Yu Liu · Chaogui Kang · Song Gao · Yu Xiao · Yuan Tian

Received: 31 August 2011 / Accepted: 5 March 2012 / Published online: 21 March 2012

Abstract Intra-urban human mobility is investigated by means of taxi trajectory data that are collected in Shanghai, China, where taxis play an important role in urban transportation. From the taxi trajectories, approximately 1.5 million trips of anonymous customers are extracted on seven consecutive days. The globally spatio-temporal patterns of trips exhibit a significant daily regularity. Since each trip can be viewed as a displacement in the random walk model, the distributions of the distance and direction of the extracted trips are investigated in this research. The direction distribution shows an NEE–SWW-dominant direction, and the distance distribution can be well fitted by an exponentially truncated power law, with the scaling exponent $\beta = 1.2 \pm 0.15$. The observed patterns are attributed to the geographical heterogeneity of the study area, which makes the spatial distribution of trajectory stops to be non-uniform. We thus construct a model that integrates both the geographical heterogeneity and distance decay effect, to interpret the observed patterns. Our Monte Carlo simulation results closely match to the observed patterns and thus validate the proposed model. According to the proposed model, in a single-core urban area, the geographical heterogeneity and distance decay effect improve each other when influencing human mobility patterns. Geographical heterogeneity leads to a faster observed decay, and the distance decay effect makes the spatial distribution of trips more concentrated.

Keywords Intra-urban human mobility · Taxi trajectory · Geographical heterogeneity · Distance decay · Monte Carlo simulation

JEL Classification C15 · R40

Y. Liu (✉) · C. Kang · S. Gao · Y. Xiao · Y. Tian
Institute of Remote Sensing and Geographical Information Systems, Beijing 100871, China
e-mail: liuyu@urban.pku.edu.cn

1 Introduction

Human mobility has become a hot research topic recently, since the wide use of location-aware devices such as GPS (global positioning system) receivers and mobile phones offers great convenience for collecting large volumes of individual trajectory data (González et al. 2008; Jiang et al. 2009; Rhee et al. 2008; Song et al. 2010a, b; Yuan et al. 2012). Cities are concentrated areas of human activities, and thus, intra-urban motion is a dominant part of life for citizens. Identifying patterns of intra-urban human mobility will help us understand urban dynamics and reveal the driving social factors, such as gender and occupation (Sang et al. 2011). Currently, location-aware devices are widely applied in urban studies (Chowell et al. 2003; Phithakkitnukoon et al. 2010; Ratti et al. 2006; Shoval 2008). In terms of mobile data, Ahas et al. (2010) investigated the movement patterns of suburban commuters of Tallinn, Estonia, using mobile positioning data and identified a remarkable temporal rhythm of respondents' locations. The motion of mobile users leads to varying traffic intensities of corresponding base stations, which can be measured using Erlang values.[1] Ratti et al. (2006) mapped the dynamics of urban activities in the metropolitan area of Milan, Italy, using the Erlang values of cell phone stations. Sevtsuk and Ratti (2010) also adopted Erlang measures in Rome, Italy, and found significant temporal regularity in human mobility. A similar study based on principal component analysis was conducted by Sun et al. (2011) using data collected in Shenzhen, China.

In addition to mobile data, bank notes (Brockmann et al. 2006), travel bugs (Brockmann and Theis 2008), and check-ins in location sharing services (Cheng et al. 2011) can also be used for understanding human mobility patterns. Recently, GPS-enabled floating cars[2] have provided an alternative approach to gathering large volumes of individual trajectories and studying individuals' behaviors and urban dynamics (Jiang et al. 2009; Liu et al. 2010; Li et al. 2011; Qi et al. 2011; Zheng et al. 2011). The floating car technique has been adopted by intelligent transportation systems (ITSs) to collect traffic information in recent years (Dai et al. 2003; Kühne et al. 2003; Lü et al. 2008; Tong et al. 2009). Each floating car periodically records its positional information, which is obtained using a GPS receiver, and sends such information to the data center. Using the collected data from a large number of floating cars, the real-time traffic status of a city can be estimated and assessed. In practice, floating cars are often served by taxis in many cities (Li et al. 2011), and thus, it is convenient to collect human mobility data. For instance, Jiang et al. (2009) analyzed trajectories of individuals, which were obtained from taxis of four cities in Sweden, and argued that the mobility pattern is determined by the street layout.

A number of mobility models have been proposed, including random way point, random direction, Brownian motion, random walk, and obstacle model for describing human movement (Lee et al. 2009). Much research has shown that the human mobility

[1] The traffic measured in Erlang values represents the average number of concurrent calls carried by a mobile phone tower. The motion of mobile users leads to varying traffic intensities of corresponding base stations, which can be measured using Erlang values.

[2] A number of types of floating car data, such as cellular network-based data and electronic toll-based data, are available at present. This research uses GPS-based floating car data.

patterns can be modeled using Lévy flight or truncated Lévy flight (Brockmann et al. 2006; Jiang et al. 2009; Rhee et al. 2008). A Lévy flight is a specific random walk model that satisfies the following two conditions: (1) the step lengths follow a power law, or a truncated power law for truncated Lévy flights, and (2) the angle distribution is uniform. The power law distribution of step lengths indicates distance decay, which widely exists in geographical phenomena. For example, Lu (2003) found a power law distance decay effect in criminals' journey-after-auto-theft in Buffalo, USA. Many geographical models, such as the gravity model, are constructed directly based on power law distance decay. In practice, it is difficult to collect sufficient data to examine whether the trajectory of a particular individual follows the Lévy flight model. Hence, the examinations are often conducted using data sets that consist of large numbers of individual trajectories, and thus, the statistics exhibit a convolution of population heterogeneity and individual motion (González et al. 2008).

A metropolitan area is a region where human activities are highly concentrated, and thus forms a relatively complete unit for analyzing human mobility patterns. Will the intra-urban human mobility patterns be different from the patterns reported in existing literature? How to interpret the observed patterns by taking into account geographical impacts? This research adopts the taxi trajectories of Shanghai, China, to address the two questions. Taxis occupy a large proportion of urban traffic services in Shanghai, and the underlying patterns in the taxi trajectories thus reflect the characteristics of human mobility. About 1.5 million trips of anonymous customers are extracted from the taxi trajectory data. Each trip is represented by a vector $\langle(x_{i1}, y_{i1}, t_{i1}), (x_{i2}, y_{i2}, t_{i2})\rangle$, where (x_{i1}, y_{i1}) and (x_{i2}, y_{i2}) denote positions where a customer was picked up and dropped off, and t_{i2} and t_{i2} are the pick-up time and drop-off time, respectively. In general, one trip is associated with a specific purpose, so that one can stay at both (x_{i1}, y_{i1}) and (x_{i2}, y_{i2}) for a period of time and continuously move between (x_{i1}, y_{i1}) and (x_{i2}, y_{i2}). Hence, such a trip can be viewed as a displacement in the random walk model of an individual.

In this research, the distance and direction distributions of intra-urban trips are focused on. The trip distances follow the exponentially truncated power law distribution, which is consistent with the findings of Brockmann et al. (2006) and González et al. (2008). The direction distribution, however, is not uniform. We conjecture that the identified patterns are influenced by geographical heterogeneity; that is, the probability that a point serves as a potential stop in a trajectory varies in geographical space. Monte Carlo simulations reproduce the observed patterns well and thus confirm the conjecture. Compared with existing studies, this research highlights the impact of geographical heterogeneity on human mobility patterns and points out that the observed decay in distance distributions should be attributed to two aspects: heterogeneous geographical space and the inherent distance decay effect associated with spatial behavior. Additionally, there is a reciprocity effect between these two aspects.

2 Data

Shanghai is the most populous city in China. Taxis play an important role in the urban transportation of Shanghai. At the end of 2009, 149 companies possessed

Table 1 Statistics of the seven-day taxi trajectories

Date	Number of records	Number of taxies	Number of trips	Number of valid trips
1 June	47,030,136	6,644	220,203	217,491
2 June	46,955,696	6,641	214,313	211,299
3 June	47,207,021	6,645	215,185	212,427
4 June	45,650,056	6,645	209,498	206,721
5 June	47,177,600	6,643	224,852	221,225
6 June	47,718,064	6,648	251,213	247,650
7 June	48,821,201	6,643	217,371	214,684
Sum	330,559,774		1,552,635	1,531,497

approximately 47,000 taxis in Shanghai Municipality. If we consider only the urban area, there are 130 companies and 43,000 taxis. In 2009, these taxis carried about three million passengers each day, occupying more than 20 % of the intra-urban travel within Shanghai.[3] Many taxi companies have their vehicles equipped with GPSs to monitor the operation of each taxi. Meanwhile, the urban government can use the taxis that are equipped with GPS receivers as “floating” cars to obtain the status of real-time traffic.

In this research, the data set records more than 6,600 floating cars of an anonymous taxi company of Shanghai. The data set spans seven consecutive days, from June 1, 2009, to June 7, 2009. For each taxicab, information on its position, velocity, and whether customers are being transported is automatically collected approximately every 10 s. Theoretically, there should be approximately 55 million records each day. However, the actual data volume, including about 47 million records, is slightly less because some taxi drivers could shut down their GPS receivers after work. Table 1 summarizes the statistics of the data set. Figure 1a demonstrates a one-day trajectory of a taxicab, where the red lines denote the trajectories when there are passengers inside the taxicab, and the blue lines indicate unoccupied statuses. Using the taxicab trajectories that explicitly record positions where anonymous passengers are picked up and dropped off (Fig. 1b, c), we extract 1,552,635 trips. In this research, each trip is simplified to be a point pair, which is represented by a pick-up point (PUP) and a drop-off point (DOP). The two points can be viewed as the origin and destination of a trip,[4] and forms a vector that represents an increment to model human mobility. It should be noted that short vectors with norms less than 0.5 km are removed as they are often caused by false operations or data transfer errors. Although the round trips are also filtered, the global patterns do not change much, since the proportions of such trips are very small (approximately 1 %) every day.

[3] According to the report of Shanghai Municipal Transport and Port Authority, http://www.jt.sh.cn/.

[4] It should be noted that all PUPs and DOPs are in streets, and people usually walk to a street for taxi services. This makes the extracted PUPs and DOPs slightly different from the actual origins and destinations. With respect to the global trips patterns, such differences do not change the distributions of distance and direction much.

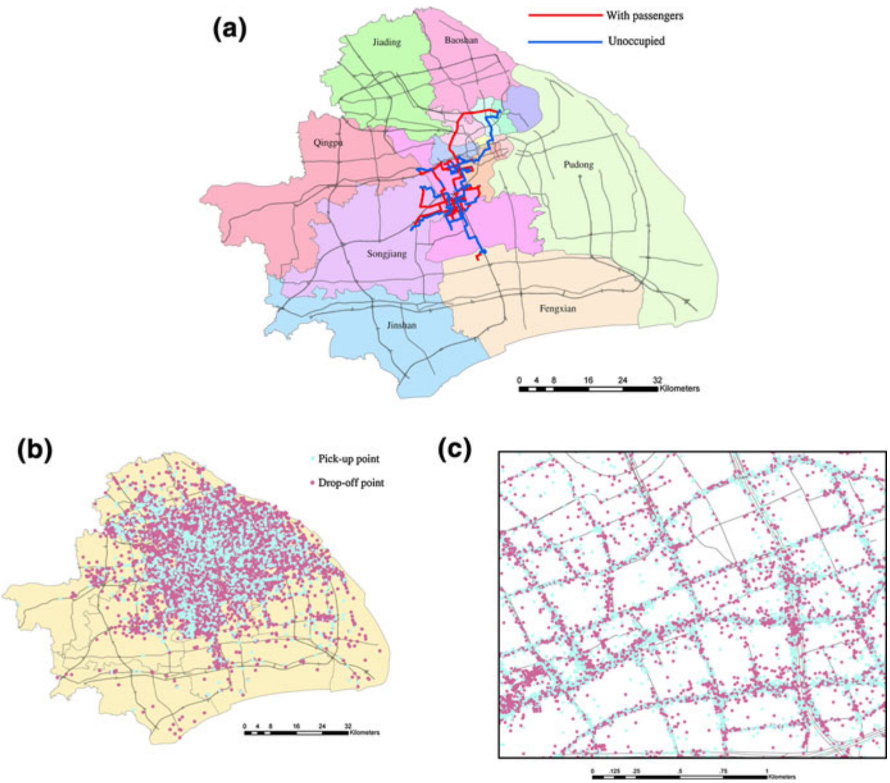

Fig. 1 **a** A one-day trajectory of a taxicab with a map of the research area, including 16 districts of Shanghai except for Chongming Island, **b** spatial distribution of PUPs and DOPs (date: 1 June), **c** detailed map of a rectangle subarea

3 Methodology

Figure 2 depicts the analysis flow chart for this paper. As each trip is simplified to a vector $\langle(x_{i1}, y_{i1}, t_{i1}), (x_{i2}, y_{i2}, t_{i2})\rangle$, the trip patterns can be analyzed from the following two aspects. First, the properties, such as distances, directions, and durations, of all trips can be computed and the associated statistical distributions are thus obtained. Second, we can investigate the temporal and spatial distributions of all trips. This research pays more attention to the distance and direction distributions, since they are extensively investigated in existing literature. The observed distributions enlighten us to construct a model incorporating both geographical heterogeneity and distance decay effect. The Monte Carlo simulation method is introduced to validate the model. In the simulations, the geographical heterogeneity is represented by the LandScan$^{\text{TM}}$ 2008 data,[5] and the distance decay effect is formulated by power functions. A great number of

[5] http://www.ornl.gov/sci/landscan/.

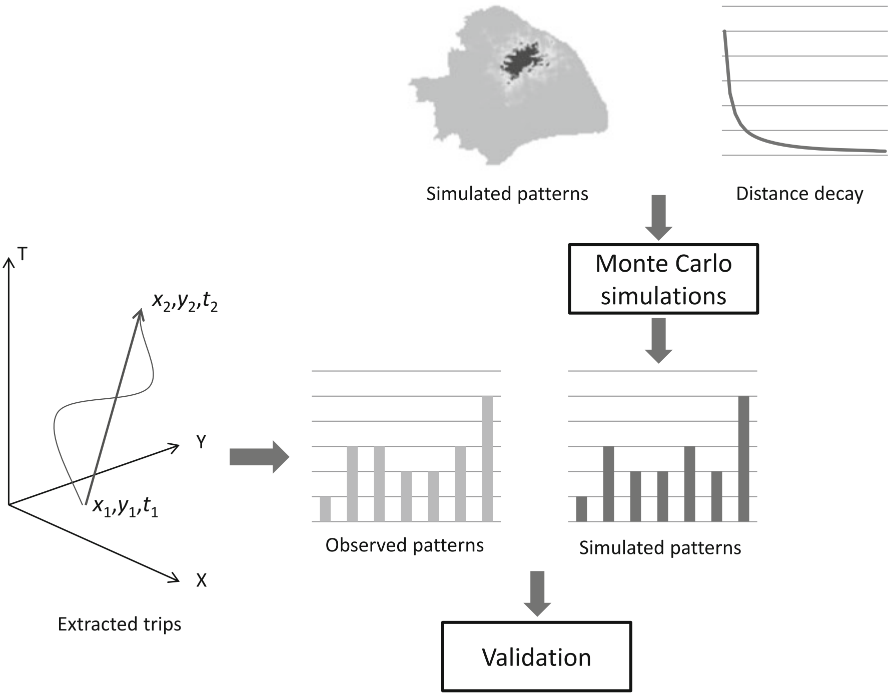

Fig. 2 Flow chart for analyzing trip patterns and validating the proposed model

synthetics trips are generated and their distance and direction distributions are computed. Different values for the exponent in distance decay functions are tried to find the best fit. If the best fit passes the statistical test, it indicates that the Monte Carlo simulations reproduce the empirical trips well and thus validate the proposed model.

4 Intra-urban trip patterns

In this research, one day is adopted as the temporal unit for analysis. Although one trip could cover 2 days, for example, one trip may originate in a taxi at 23:50 on one day and terminate at 0:15 of the next day, the proportion of such trips is very low (less than 0.1 %). Hence, we simply discard such trips and focus on the temporal and spatial characteristics of the extracted trips using the taxi trajectories.

4.1 Temporal distribution of PUPs and DOPs

Since a trip lasts for a period of time, it is difficult to compute the temporal distribution of the trips directly. However, the occurrences of pick-ups and drop-offs during each hour can be obtained easily. This distribution indicates the temporal

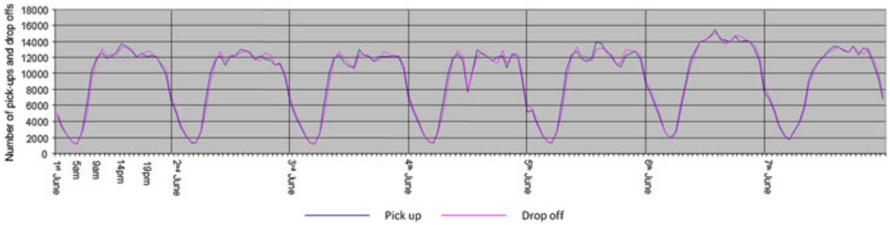

Fig. 3 Number of pick-ups and drop-offs in one hour and their temporal variation during the seven-day period

variation in human activities during a period of time and exhibits a strong daily rhythm (Fig. 2), a remarkable finding observed in many previous studies (Ahas et al. 2010; Schonfelder and Axhausen 2010). As shown in Fig. 3, the temporal patterns over the 7 days are quite similar. Meanwhile, people take more trips during the day than at night. In each day, especially during the weekdays, three peaks can be identified at approximately 9:00, 14:00, and 19:00, which generally correspond to the activities of going to work, going to lunch, and going home. The lowest point appears to be at approximately 5:00. If we define a cycle from 5:00 of one day to 5:00 of the next day, the curve inside a cycle is roughly symmetric. Such a temporal pattern of activities is similar to those identified from mobile phone call records (Candia et al. 2008; Sevtsuk and Ratti 2010). It should be noted that the temporal patterns on Saturday and Sunday are different from those on weekdays. On weekends, especially on Saturday, entertainment and shopping constitute a large proportion of the trip purposes, and the number of trips to and from work is relatively low. Hence, there are more taxi trips on Saturday, and the three peaks are not very clear. This research focuses on the distance and direction distributions of the trips and does not consider the temporal variations because the distributions are quite similar for the 7 days (cf. Table 1). There is substantial literature on this issue (Hanson and Huff 1982; Huff and Hanson 1986; Kang and Scott 2010; Susilo and Kitamura 2005), and we plan to investigate the temporal trip patterns using a data set that covers a relatively long period, such as 10 weeks.

4.2 Distribution of trip directions

Each trip is simplified to be a vector in this research, and the direction of the trip is calculated consequently. As shown in Fig. 4, the direction distributions over the 7 days are very similar.

The Hellinger coefficient is used to measure the similarity of two distributions (Vegelius et al. 1986). Suppose that the probability density functions of two continuous distributions are $p(x)$ and $q(x)$, which are defined over the same domain X. Then, the Hellinger coefficient is given by the following:

$$R_H = \int \sqrt{p(x)q(x)}dx \qquad (1)$$

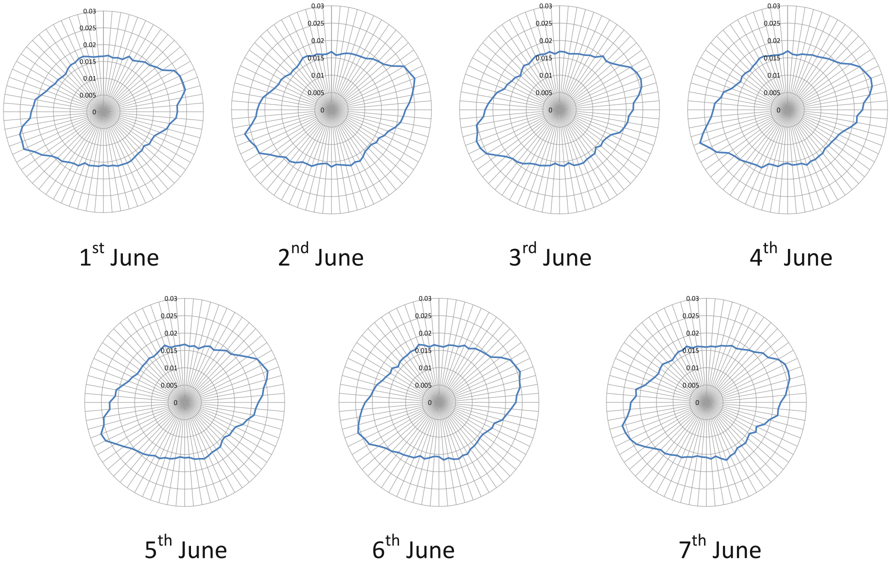

1st June 2nd June 3rd June 4th June

5th June 6th June 7th June

Fig. 4 Direction distributions of trips over the 7 days

For discrete distributions, the equation turns to be

$$R_H = \sum_{x \in X} \sqrt{p(x)q(x)} \tag{2}$$

Table 2 lists the Hellinger coefficients among the direction distributions over 7 days. The coefficient between every pair of days is greater than 0.999, indicating a high similarity between the mobility patterns of 2 days.

Two facts can be ascertained from Fig. 4. First, all of the distributions are roughly centrally symmetric. The one-day movements of most of the individuals can be viewed as round trips, in which an individual usually travels away from home in the morning and returns home in the afternoon (or evening) of each day. This fact leads to the central symmetry of the global distribution of trip directions. Second, the

Table 2 Hellinger coefficients between the direction and distance distributions of the 7 days

	1 June	2 June	3 June	4 June	5 June	6 June	7 June
1 June	1	0.99989	0.99983	0.99982	0.99978	0.99971	0.99977
2 June	0.99990	1	0.99990	0.99988	0.99991	0.99959	0.99956
3 June	0.99991	0.99991	1	0.99996	0.99989	0.99940	0.99945
4 June	0.99993	0.99991	0.99993	1	0.99992	0.99940	0.99942
5 June	0.99993	0.99991	0.99993	0.99993	1	0.99953	0.99941
6 June	0.99992	0.99991	0.99989	0.99989	0.99992	1	0.99980
7 June	0.99989	0.99991	0.99987	0.99989	0.99993	0.99991	1

The values in the upper right and lower left part of the table are Hellinger coefficients between the distance distributions and direction distributions, respectively angle distributions are not uniform, with two major directions: northeast east (NEE) and southwest west (SWW).

4.3 Distribution of trip distances

The distance distributions of the extracted trips in the 7 days are plotted in Fig. 5. Obviously, the seven curves are also very similar, and the corresponding Hellinger coefficients are all greater than 0.999 (cf. Table 2).

As mentioned earlier, each trip can be viewed as a displacement in an individual's trajectory. If human trajectories can be modeled by Lévy flights, then the statistics that are observed in the trips should exhibit a convolution of the population heterogeneity and individual motions, similar to the bank notes trajectories reported by Brockmann et al. (2006) (González et al. 2008). Hence, the trip length d follows an exponentially truncated power law distribution, as follows:

$$P(d) \sim (d + d_0)^{-\beta} \exp(-\alpha d) \tag{3}$$

In this research, the distance distribution of all trips within the 7 days can be fitted well when $\beta = 1.2 \pm 0.15$, $d_0 = 0.31$ km, and $\alpha = 0.1\ \mathrm{km}^{-1}$ (Fig. 6a). The exponent is less than 1.59 and 1.75, the values observed by Brockmann et al. (2006) and González et al. (2008), respectively.

The statistical validation is conducted using the method adopted by González et al. (2008). The computation is based on the Kolmogorov–Smirnov (KS) statistic, which is given by the following:

$$KS = \sup_x (F_1(x) - F_2(x)) \tag{4}$$

where $F_1(x)$ and $F_2(x)$ are the cumulative distribution functions of the two data sets. The KS value between the observed distribution and its best fit is 0.041. We then generate 1,000 synthetic data sets from Eq. 3 and computed the KS values. If the KS

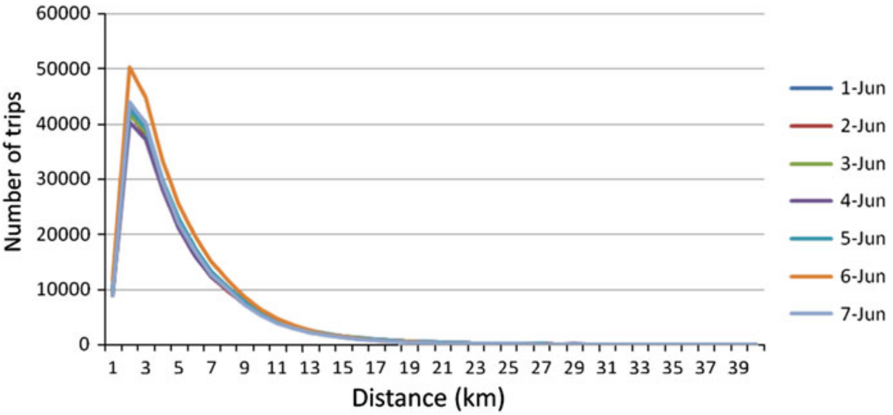

Fig. 5 Distance distributions of trips over the 7 days

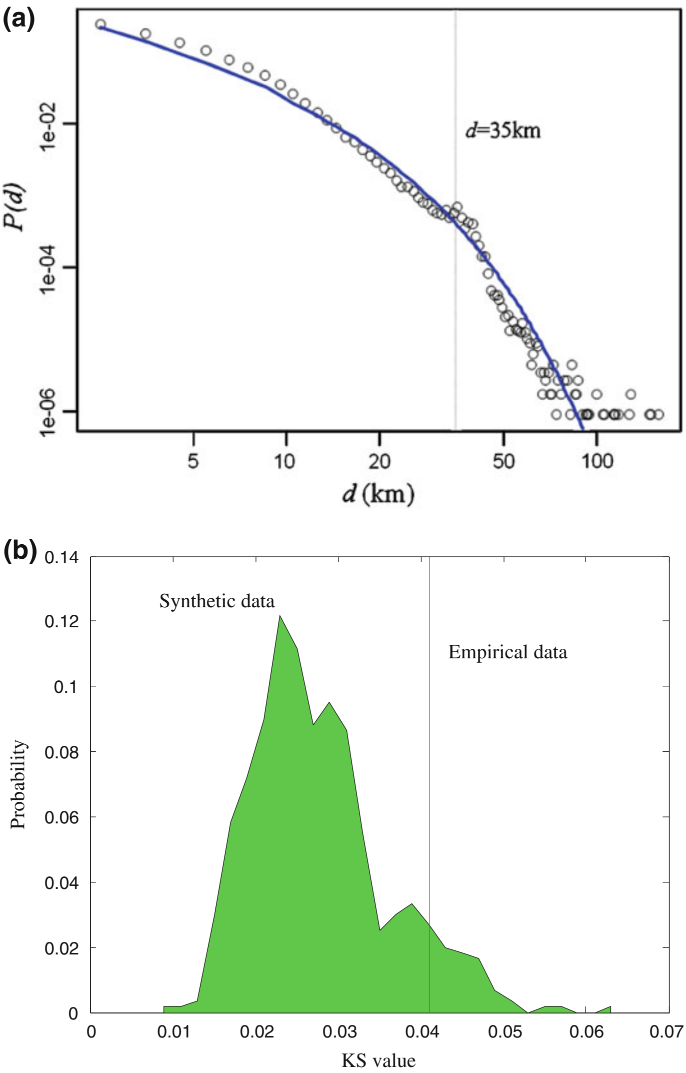

Fig. 6 **a** Log–log plot of the distance distribution of trips and the best fit to this distribution. In this plot, we removed the trips that are less than 2 km (cf. the curve left of the peak in Fig. 3). **b** KS test for the distance distribution of trips

statistics for the empirical data are equal to or less than those obtained from the synthetic data, then it can be concluded that the observed distribution is consistent with the best fit (Fig. 6b). A p-value can be computed using the distribution of the KS values generated with the synthetic data. In this statistical validation, the p-value is 0.082, indicating that the observed distance distribution passed the KS test.

In Fig. 6a, there is a small peak at approximately $d = 35$ km. This peak should be attributed to the Pudong International Airport's location, which is more than 30 km away from the downtown area of Shanghai. This location increases the

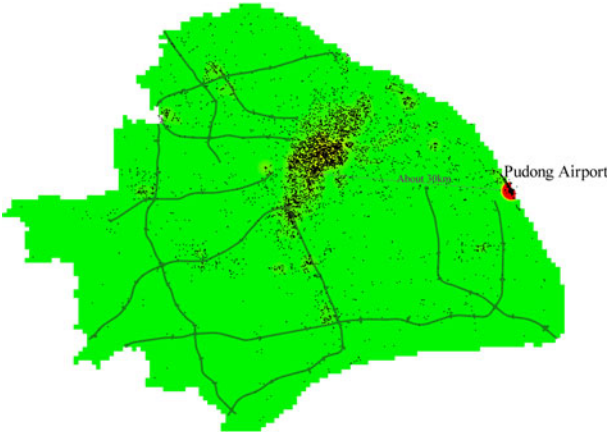

Fig. 7 The PUPs and DOP distributions of trips with lengths between 30 and 40 km

probabilities around 35 km and leads to the peak. This fact can be further confirmed by Fig. 7, which depicts the spatial distribution of the PUPs and DOPs associated with trips between 30 and 40 km. The Pudong Airport is a clear “hot” spot in Fig. 7, serving as an important attraction for generating trips within this distance interval.

4.4 Spatial distribution of PUPs and DOPs

As shown in Fig. 7, the spatial distribution of PUPs and DOPs is visualized by using kernel density analysis. The resulting maps represent the density of human activities (Table 3). The spatial distributions of both PUPs and DOPs are similar over the 7 days. The similarities can be measured using Pearson’s correlation coefficients between 2 days (Table 4). Tables 3 and 4 further confirm that the taxi-based trips exhibit stable spatio-temporal patterns. It should be noted that the maps in Table 3 are obtained with a radius of 100 m. The radius parameter in kernel density analysis will influence the correlation coefficients. Since this research addresses only the distribution similarity between the PUPs and DOPs, and the correlation coefficients are quite high (>0.98), we do not attempt to use other kernel values. Hence, we aggregate the spatial distributions of PUPs and DOPs over the 7 days into two data sets, D_u and D_o, and find that the correlation coefficient between them is 0.9927. This high correlation coefficient is natural because the probabilities that one locality serves as both an origin and a destination are roughly equal in the daily scale. If we focus on a relatively short period, for example, morning, then the distributions of the PUPs and DOPs will be significantly different.

In the daily scale, the trip distribution is in general positively correlated with the population density of the study area. This research adopts the LandScan data set to compute the population density map, denoted by D_p (Fig. 8). The spatial resolution of the original data is $30'' \times 30''$. As shown in Fig. 8, the built-up areas have a high population density. The correlation coefficients between D_u versus D_p and D_o versus

Table 3 Spatial distributions of PUPs and DOPs over the 7 days exhibit high positive correlations with population density

Date	Pick up points	Drop off points
1st June	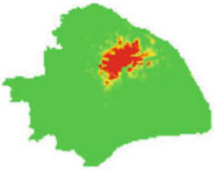	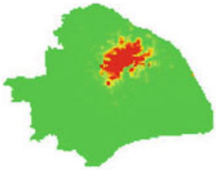
2nd June	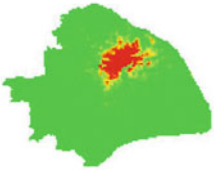	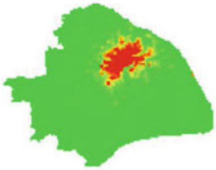
3rd June	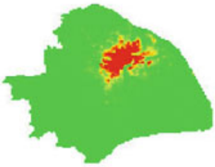	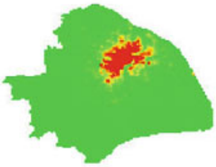
4th June	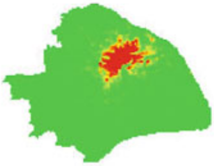	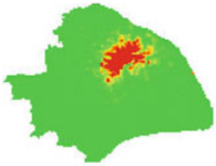
5th June	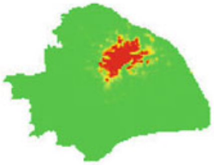	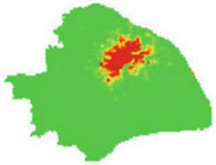
6th June	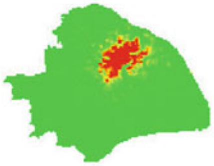	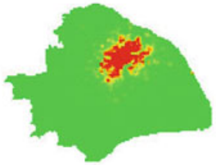
7th June	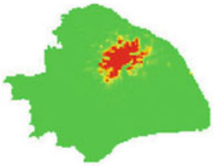	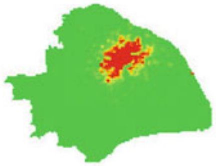

Table 4 Correlation coefficients of PUP and DOP distributions over the 7 days

	1 June	2 June	3 June	4 June	5 June	6 June	7 June
1 June	1	0.99699	0.99712	0.99642	0.99692	0.99178	0.98938
2 June	0.99720	1	0.99835	0.99817	0.99695	0.98785	0.98619
3 June	0.99698	0.99817	1	0.99903	0.99652	0.98743	0.98623
4 June	0.99676	0.99800	0.99911	1	0.99548	0.98626	0.98493
5 June	0.99753	0.99771	0.99769	0.99720	1	0.99230	0.98945
6 June	0.99234	0.98887	0.98758	0.98678	0.99123	1	0.99607
7 June	0.99276	0.99050	0.98968	0.98930	0.99107	0.99697	1

The values in the upper right matrix are coefficients between PUP distributions of two different days, and the lower left matrix represents coefficients for DOP distributions

D_p are 0.7886 and 0.7864, respectively, indicating a similar spatial pattern between the trips and the population density.

Comparing the maps in Table 3 and the population distribution in detail, the PUPs and DOPs are more concentrated than the population distribution. According to the population distribution map, a number of towns with high density generate relatively few trips. Due to the high similarity between D_u and D_o, we compute $D_u + D_o$, denoted by D_{uo}, to represent the trip distribution. D_{uo} and D_p are normalized to D'_{uo} and D'_p for the purpose of making a comparison. The normalization equations are $D'_{uo} = D'_{uo}/\sum D'_{uo}$ and $D'_p = D'_p/\sum D'_p$. Figure 9 depicts $D'_{uo} - D'_p$, and it can be clearly seen that the trip distribution is more concentrated.

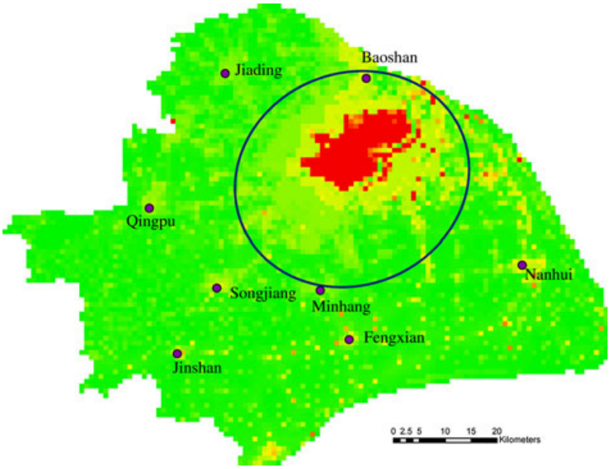

Fig. 8 LandScan™ 2008 Population density map of Shanghai. The *blue ellipse*, calculated using directional distribution analysis, represents the dominant elongation direction of the urban area (color figure online)

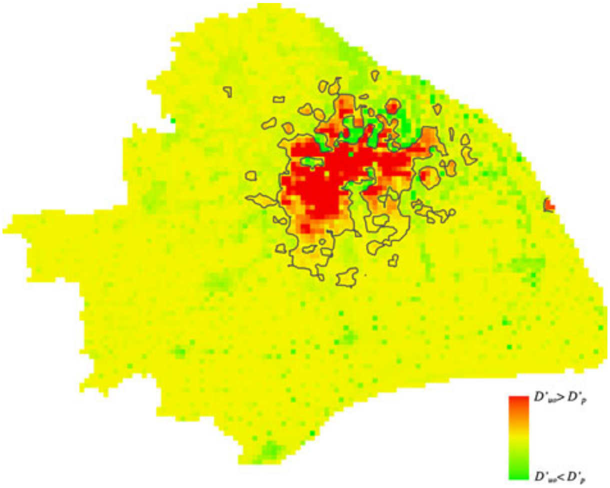

Fig. 9 The map of $D'_{uo} - D'_p$, where the gray lines denote locations where $D'_{uo} = D'_p$

5 Model and validation

5.1 Model

The trip patterns can be further investigated in detail from the following two perspectives. First, the direction distribution is not uniform. The frequencies of trips ahead to NEE and SWW are higher than those ahead to other directions. Second, the trip distribution is more concentrated than the population distribution. The geographical heterogeneity, which makes the trip distribution non-uniform, is the main factor that leads to the above two patterns.

First, as mentioned by Rhee et al. (2008) and Jiang et al. (2009), the anisotropic trip distribution is usually caused by geographical constraints, such as the street network. In this research, since all trips are simplified to vectors, the street network does not affect the angle distributions and the urban shape becomes the major factor that influences the distribution of trip directions inside the city. As shown in Fig. 10a, if a city extends along the east–west direction, then the trips with similar directions are dominant. As shown in Fig. 10a, the main elongation direction of the Shanghai urban area is NEE–SWW, which shapes the direction distribution of trips.

Second, the urban form also affects the distance distribution of the trips. Intuitively, human activities, as well as trips, would be highly concentrated in the urban area, and the probability of long-distance trips would be lower. Figure 10b illustrates an extreme example of this point. If a city is shaped as a circle with a diameter of 1 km, and all trips are restricted to be inside the urban area, then obviously, $Pr(d > 1\text{ km}) = 0$. Hence, the low probabilities of long-distance trips are caused by two aspects: the distance decay of each individual's motion and the geographical heterogeneity.

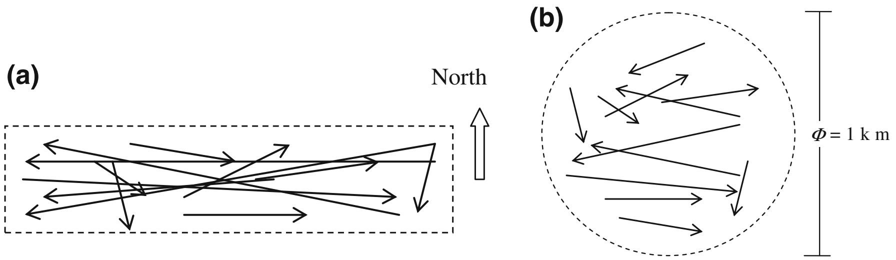

Fig. 10 Urban shape influences the direction and distance distribution of trips inside an imaginary city, the boundary of which is depicted by the *dashed line*

In the conventional Lévy flight model, the distance decay effect is represented by a power law function. However, geographical heterogeneity is not taken into account; thus, the probabilities that all point in the study area serves as the stops of a trajectory are equal. In practice, one could visit several points frequently (Song et al. 2010a, b) or visit specific regions with higher probabilities due to geographical heterogeneity. This research constructs a model that integrates geographical heterogeneity. Let $\boldsymbol{S}$ denote the set of potential stops in the individuals' trajectories, and $z = f(x, y)$ be a field representing geographical heterogeneity. The spatial distribution of $\boldsymbol{S}$ is positively correlated with z. We thus have

$$P_S(x, y) \propto f(x, y) \tag{5}$$

where $P_s(x, y)$ represents the probability that the point (x, y) serves as a stop. Hence, the distributions of potential PUPs and DOPs are both positively correlated with $P_s(x, y)$. On the other hand, $f(x, y)$ is usually determined by the spatial distribution of the land uses and the population of a city. Under the constraint of $f(x, y)$, a number of point pairs can be generated. Each point pair $(x_1, y_1) - (x_2, y_2)$ could be an actual trip with a particular probability, which is mainly dependent on the distance between the two points. Suppose the distance is d, and the distance decay is represented by $g(d)$, we have

$$P_T(T|(x_1, y_1, x_2, y_2)) \propto g(d) \tag{6}$$

where $P_t(T|(x_1, y_1, x_2, y_2))$ is the conditional probability that there is a trip between (x_1, y_1) and (x_2, y_2) given that (x_1, y_1) and (x_2, y_2) are two stops. Hence,

$$P_T(T_{(x_1,y_1)\to(x_2,y_2)}) \propto f(x_1, y_1)f(x_2, y_2)g(d) \tag{7}$$

and the final trip patterns are determined by $f(x,y)$ and $g(d)$.

5.2 Model validation

Following the proposed model, Monte Carlo simulation is adopted to reproduce the observed human mobility patterns. If the simulation results fit the real distributions well, then we can argue that the model is well grounded. Such an approach has been widely used in existing literature (González et al. 2008; Jiang et al. 2009; Song et al. 2010a). The LandScan$^{\text{TM}}$ population distribution data are used to represent geographical heterogeneity in this research. In other words, the densities of the potential PUPs and DOPs are positively correlated with the population density. Meanwhile, the power law distance decay is adopted, as follows:

$$g(d) = (d + d_0)^{-\beta_d} \tag{8}$$

where d_0 is the cutoff distance and β_d denotes the degree of distance decay in the behavior associated with taking taxis. In the Monte Carlo simulations, generating a synthetic trip includes three steps. First, a starting point is determined based on the population density, using the method proposed in Liu et al. (2009). Second, the candidate destination is generated following $g(d)$ and a uniform direction distribution. Finally, the acceptance-rejection method (Robert and Casella 2004) is adopted to determine whether the obtained point pair should be accepted as an actual trip according to the distribution of the population density. It should be noted that the model does not take into account population heterogeneity, because all trips are generated using the same $g(d)$.

To make a comparison with the best fit function, d_0 is set to 0.31 km. Different exponent values between 1.0 and 2.0 are tried, and 1,000,000 trips are generated for each exponent. The observed distance distribution can be best fitted when $\beta_d = 1.08$. Figure 11a demonstrates the statistical validation. By setting $\beta_d = 1.08$, we compute the distance and direction distributions of generated trips and compared them with those of the empirical data (Fig. 11b, c). The Hellinger coefficients for distance and direction distributions are 0.9959 and 0.9993, indicating that the proposed model interprets the observed human mobility pattern well.

5.3 Further analyses

If human mobility is strictly modeled by Lévy flights, then the direction distribution would be expected to be uniform, that is, the observed human mobility patterns would be isotropic. However, due to the geographical heterogeneity, the probabilities that one person moves to the next points with the same distance but in different directions are different for a given starting point. The proposed model and the associated Monte Carlo simulation reveal such anisotropy. The model validation also indicates that the population density distribution is an important factor that constrains human mobility.

As shown in Fig. 7, there is a connected urban area with a high population density. Most trips are constrained inside it, which leads to a probability decrease in long-distance trips in addition to the decreased probability that is caused by the distance decay effect. Meanwhile, due to the distance decay effect, the probabilities of short-distance trips are relatively high, which makes the trip distribution more concentrated in the urban area than that represented by the population density.

To clearly demonstrate the above arguments, we introduce a Gaussian surface (Fig. 12a) to represent geographical heterogeneity and run the simulation to generate synthetic trips following a power law distance decay, that is, $g(d) = \mathrm{d}^{-\beta}$. Three data sets, D_1, D_2, and D_3, are obtained using $\beta_{d1} = 1.1$, $\beta_{d2} = 1.5$, and $\beta_{d3} = 2.0$, respectively. For each exponent, we run 20 simulations and generate

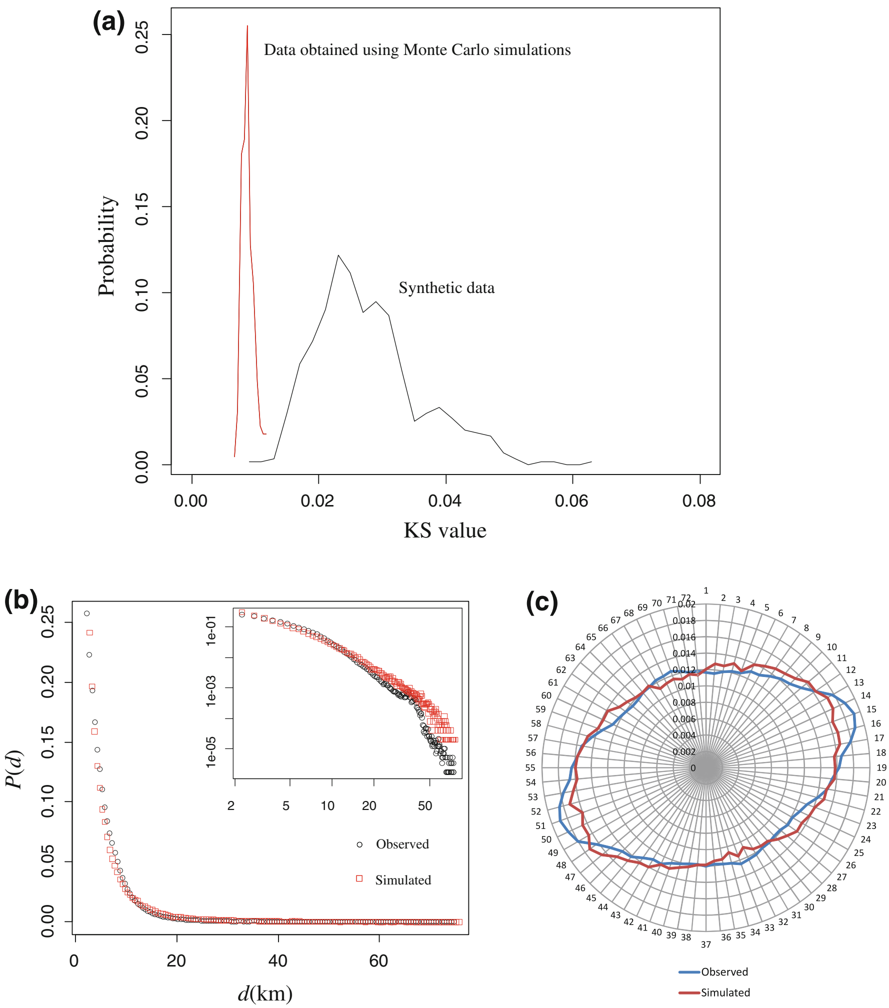

Fig. 11 **a** KS test for the trips generated using Monte Carlo simulation. It should be noted that the vertical units of the two curves are not in proportion and the Y-axis is for the synthetic data. **b** Distance distributions of observed trips and simulated trips, **c** direction distributions of observed trips and simulated trips

100,000 trips in total. As shown in Fig. 12b, the observed distance distributions have “thinner tails” than those of corresponding power laws, suggesting faster decay when considering geographical heterogeneity. D_1, D_2, and D_3 can all be well fitted by truncated power laws $p(x) \propto x^{-\beta}\exp(-\alpha x)$, where $\beta_1 = 1.3$, $\alpha_1 = 0.065$; $\beta_2 = 1.54$, $\alpha_2 = 0.067$; and $\beta_3 = 1.97$, $\alpha_3 = 0.058$, respectively. For the Gaussian surface, β roughly equals β_d such that the term $\exp(-\alpha x)$ is derived mainly from geographical heterogeneity. We also investigate the spatial distribution of the synthetic trips. Figure 12c depicts all DOPs and PUPs generated in one pass of the simulation based on β_{d3}. The point density in each 1-km circular band centered at

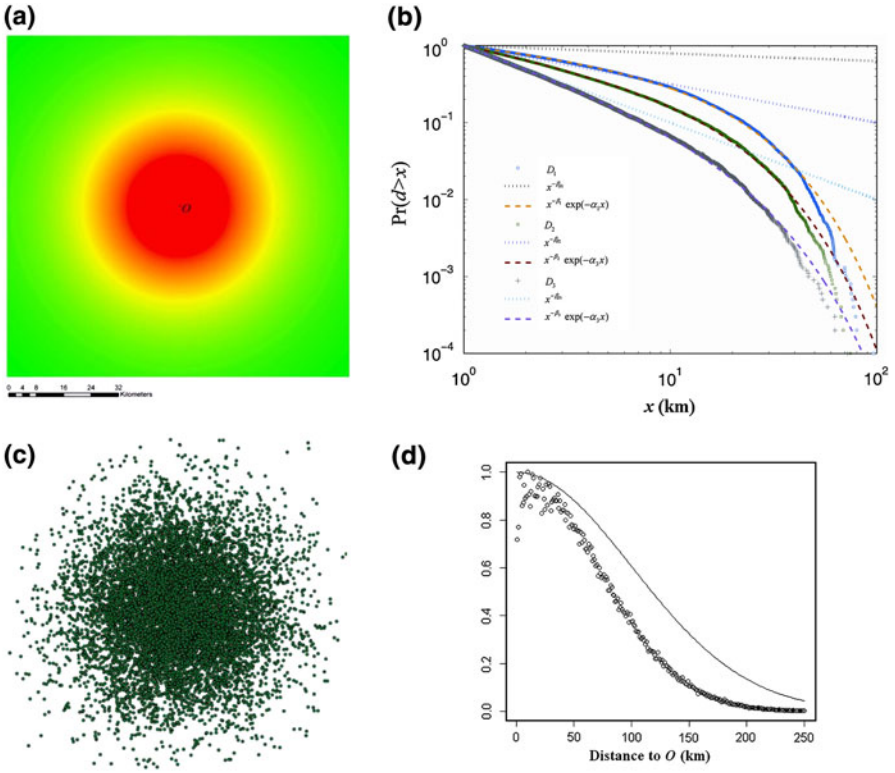

Fig. 12 **a** A Gaussian surface representing geographical heterogeneity; **b** cumulative distance distributions of trips generated following Gaussian heterogeneity and power law distance decay, where different exponents were adopted; **c** 10,000 PUPs and DOPs generated in one pass of simulation using the exponent 2.0; **d** normalized point densities in 1-km circular bands, which demonstrates a more concentrated pattern than the Gaussian surface

O can thus be computed. Figure 12d plots the relationship between the normalized densities and the band radii. A profile of the Gaussian surface from O to its edge is also drawn as a comparison. The spatial distribution of the simulated trips is more concentrated than the Gaussian surface. This result is consistent with the second finding mentioned in Sect. 4.4 (cf. Fig. 9).

6 Conclusions

This research uses a trajectory data of GPS-equipped taxis in Shanghai, China, to extract a large volume of trips of anonymous customers and to identify the patterns of intra-urban human mobility. The spatio-temporal distribution of the trips exhibits a strong daily rhythm and the patterns of the 7 days are stable (cf. Figs. 2, 3, and 6, and Tables 1 and 2). Hence, the data set is an unbiased sample of taxi-based motion of Shanghai citizens. Each trip is represented by a point pair and can be viewed as a displacement in the random walk model.

We examine the distance and direction distributions of all extracted trips in this study. The direction distribution is not uniform and has NEE–SWW as a major direction, and the distance distribution can be fitted by an exponentially truncated power law. To investigate the identified patterns, the LandScan^{TM} population density map is introduced to offer a global constraint to the spatial distribution of the trips. Hence, given two points, the probability that there is a trip between them depends on the population densities at the two points and the distance between them, which represent geographical heterogeneity and distance decay, respectively. These two aspects together influence the observed human mobility patterns. A number of Monte Carlo simulations are run to generate synthetic trips, so that we can compute the distance and direction distributions and compare them with observed distributions. The comparison indicates that the proposed model interprets well the observed patterns. This research achieves two findings. First, the major trip direction is identical to the main elongation direction of the urban area. Second, the distance distribution can be matched well when the power law distance decay ($d^{-1.08}$) is adopted. The exponent 1.08 indicates the inherent distance decay effect of taxi-based trips. The observed decay $d^{-1.2}\exp(-0.01d)$, however, has a “thinner tail” than that of $d^{-1.08}$, according to the trip distance distribution. These two aspects can both be attributed to the geographical heterogeneity in the study area. In most intra-urban human mobility studies, we can generally find one core urban area, which shapes the direction distribution and enhances the distance decay observed in the distance distribution. Nevertheless, the distance decay effect makes the spatial distribution of the trips more concentrated. In summary, the geographical heterogeneity and distance decay effect together influence the actual human mobility patterns. Such an interaction is confirmed by a simulation based on Gaussian geographical heterogeneity.

Compared with existing human mobility research based on the assumption that the space is homogeneous, this research highlights the importance of geographical heterogeneity in shaping the intra-urban human mobility. However, the population heterogeneity is not considered in this research, since long-term individual trajectories cannot be collected using the taxi data to measure the population heterogeneity effect. Although the proposed model interprets the observed patterns well, population heterogeneity should not be neglected. Shanghai has socio-spatial differentiation on the subdistrict level in terms of attributes of employment sectors such as the primary sector, secondary sector, and service sector, as well as migrant status and educational attainment. The spatial distribution of residents working in different employment sectors exhibits a concentric pattern, with the tertiary sector concentrated in the downtown area (Li et al. 2007). Undoubtedly, employees in different sections have different motion characteristics. These trends indicate that population heterogeneity and geographical heterogeneity are tightly coupled. In the future, we plan to use more detailed trajectory data to decouple the two types of heterogeneity. To address the geographical heterogeneity, this research adopts population density and finds that it is positively correlated with trip distributions. However, some regions have low population density but relatively high trip distributions. A good example is the Pudong Airport (cf. Fig. 7). It is reasonable that many public facilities, such as railway stations, airports, and parks, attract more trips than those estimated according to the population density. In future research, we plan to introduce the distribution of POIs (point of interest) to investigate the spatial characteristics of trips. A feasible approach is to estimate *f*(*x*, *y*), the field influencing the probability that one point serves as a trajectory stop, using the reverse gravity model (O'Kelly et al. 1995). The difference between *f*(*x*, *y*) and the population distribution can be explained using the POI distributions.

Lastly, it should be noted that taxi data inevitably encounter issues of representativeness, that is, mobile users and taxi passengers are not random samples of the population. Another representativeness issue of the taxi data is that one could choose different transportation modes, such as driving private vehicles, taking a bus or subway, or taking a taxi for various trip purposes. It is natural that different modes are associated with different patterns. For example, the exponents representing the distance decay effect would be different. Hence, further investigation is in need to generalize the patterns identified from taxi-based trips.

Acknowledgments This research is supported by NSFC (Grant nos. 40928001 and 41171296) and the National High Technology Development 863 Program of China (Grant nos. 2011AA120301 and 2011AA120303).

References

Ahas R, Aasa A, Silm S, Tiru M (2010) Daily rhythms of suburban commuter's movements in the Tallinn metropolitan area: case study with mobile positioning data. Transport Res C Emer 18(1):45–54

Brockmann D, Theis F (2008) Money circulation, trackable items, and the emergence of universal human mobility patterns. IEEE Pervas Comput 7(4):28–35

Brockmann D, Hufnagel L, Geisel T (2006) The scaling laws of human travel. Nature 439:463–465

Candia J, González MC, Wang P, Schoenharl T, Madey G, Barabási A-L (2008) Uncovering individual and collective human dynamics from mobile phone records. J Phys A Math Theor 41(22):224015(1–11)

Cheng ZY, Caverlee J, Lee K, Sui DZ (2011) Exploring millions of footprints in location sharing services. ICWSM 2011:81–88

Chowell G, Hyman JM, Eubank S, Castillo-Chavez C (2003) Scaling laws for the movement of people between locations in a large city. Phys Rev E 68(6):066102(1–7)

Dai X, Ferman MA, Roesser RP (2003) A simulation evaluation of a real-time traffic information system using probe vehicles. ITSC 1:475–480

González MC, Hidalgo CA, Barabási A-L (2008) Understanding individual human mobility patterns. Nature 453:779–782

Hanson S, Huff J (1982) Assessing day to day variability in complex travel patterns. Transp Res Rec 891:18–24

Huff J, Hanson S (1986) Repetition and variability in urban travel. Geogr Anal 18(3):97–114

Jiang B, Yin J, Zhao S (2009) Characterizing the human mobility pattern in a large street network. Phys Rev E 80(2):021136(1–11)

Kang H, Scott DM (2010) Exploring day-to-day variability in time use for household members. Transport Res A Pol 44(8):609–619

Kühne R, Schäfer R-P, Mikat J, Thiessenhusen K-U, Böttger U, Lorkowski S (2003) New approaches for traffic management in metropolitan areas. IFAC CTS 2003 symposium, Tokyo, Japan, 4–6 Aug

Lee K, Hong S, Kim SJ, Rhee I, Chong S (2009) SLAW: a mobility model for human walks. IEEE INFOCOM 2009, pp 855–863

Li Z, Wu F, Gao X (2007) Global city polarization and socio-spatial restricting in Shanghai. Sci Geogr Sinica 27(3):304–311

Li Q, Zhang T, Wang H, Zeng Z (2011) Dynamic accessibility mapping using floating car data: a network-constrained density estimation approach. J Transp Geogr 19(3):379–393

Liu Y, Guo Q, Wieczorek J, Goodchild MF (2009) Positioning localities based on spatial assertions. Int J Geogr Inf Sci 23(11):1471–1501

Liu L, Andris C, Ratti C (2010) Uncovering cabdrivers' behaviour patterns from their digital traces. Comput Environ Urban 34(6):541–548

Lu Y (2003) Getting away with the stolen vehicle: an investigation of journey-after-crime. Prof Geogr 55(4):422–433

Lü W, Zhu T, Wu D, Dai H, Huang J (2008) A heuristic path-estimating algorithm for large-scale real-time traffic information calculating. Sci China Ser E 51(S1):165–174

O'Kelly ME, Song W, Shen G (1995) New estimates of gravitational attraction by linear programming. Geogr Anal 27(4):271–285

Phithakkitnukoon S, Horanont T, Lorenzo GD, Shibasaki R, Ratti C (2010) Activity-aware map: Identifying human daily activity pattern using mobile phone data. HBU 2010 LNCS 6219, pp 14–25

Qi G, Li X, Li S, Pan G, Wang Z, Zhang D (2011) Measuring social functions of city regions from large-scale taxi behaviors. IEEE PERCOM Workshops, pp 384–388

Ratti C, Pulselli RM, Williams S, Frenchman D (2006) Mobile landscapes: using location data from cell phones for urban analysis. Environ Plann B 33(5):727–748

Rhee I, Shin M, Hong S, Lee K, Chong S (2008) On the levy-walk nature of human mobility. IEEE INFOCOM, pp 924–932

Robert CP, Casella G (2004) Monte Carlo statistical methods, 2nd edn. Springer, New York

Sang S, O'Kelly M, Kwan M-P (2011) Examining commuting patterns: results from a journey-to-work model disaggregated by gender and occupation. Urban Stud 48(5):891–909

Schonfelder S, Axhausen KW (2010) Urban rhythms and travel behaviour: spatial and temporal phenomena of daily travel. Ashgate Publishing, London

Sevtsuk A, Ratti C (2010) Does urban mobility have a daily routine? Learning from the aggregate data of mobile networks. J Urban Technol 17(1):41–60

Shoval N (2008) Tracking technologies and urban analysis. Cities 25(1):21–28

Song C, Koren T, Wang P, Barabási A-L (2010a) Modelling the scaling properties of human mobility. Nat Phys 6(10):818–823

Song C, Qu Z, Blumm N, Barabási A-L (2010b) Limits of predictability in human mobility. Science 327(5968):1018–1021

Sun J, Yuan J, Wang Y, Si H, Shan X (2011) Exploring space–time structure of human mobility in urban space. Phys A 390(5):929–942

Susilo YO, Kitamura RK (2005) Analysis of the day-to-day variability in the individual's action space: an exploration of the six-week mobidrive travel diary data. Transp Res Rec 1902:124–133

Tong D, Coifman B, Merr CJ (2009) New perspectives on the use of GPS and GIS to support a highway performance study. T GIS 13(1):69–85

Vegelius J, Janson S, Johansson F (1986) Measures of similarity between distributions. Qual Quant 20(4):437–441

Yuan Y, Raubal M, Liu Y (2012) Correlating mobile phone usage and travel behavior: a case study of Harbin, China. Comput Environ Urban 36(2):118–130

Zheng Y, Liu Y, Yuan J, Xie X (2011) Urban computing with taxicabs. UbiComp 2011, pp 17–21